

PAPER • OPEN ACCESS

Role of external neutrons of weakly bound nuclei in reactions with their participation

To cite this article: M A Naumenko *et al* 2018 *J. Phys.: Conf. Ser.* **1023** 012018

View the [article online](#) for updates and enhancements.

Related content

- [Nuclear Materials Science: Atomic considerations](#)
K Whittle

- [8Be and 9B nuclei in dissociation of relativistic 10B and 11C nuclei](#)
D A Artemenkov, V Bradnova, E Firu et al.

- [INNER CRUSTS OF NEUTRON STARS IN STRONGLY QUANTIZING MAGNETIC FIELDS](#)
Rana Nandi, Debades Bandyopadhyay, Igor N. Mishustin et al.

Role of external neutrons of weakly bound nuclei in reactions with their participation

M A Naumenko¹, Yu E Penionzhkevich^{1,2}, V V Samarin^{1,3}, and Yu G Sobolev¹

¹ Flerov Laboratory of Nuclear Reactions, Joint Institute for Nuclear Research, Dubna, Moscow Region, 141980, Russian Federation

² Department of Experimental Methods in Nuclear Physics, National Research Nuclear University MEPhI, Moscow, Moscow Region, 115409, Russian Federation

³ Department of Nuclear Physics, Dubna State University, Dubna, Moscow Region, 141982, Russian Federation

E-mail: anaumenko@jinr.ru

Abstract. The paper presents the results of measurement of the total cross sections for reactions $^{4,6}\text{He}+\text{Si}$ and $^{6,7,9}\text{Li}+\text{Si}$ in the beam energy range 5–50 A MeV. The enhancements of the total cross sections for reaction $^6\text{He}+\text{Si}$ compared with reaction $^4\text{He}+\text{Si}$ and $^9\text{Li}+\text{Si}$ compared with reactions $^{6,7}\text{Li}+\text{Si}$ have been observed. The performed microscopic analysis of total cross sections for reactions $^6\text{He}+\text{Si}$ and $^9\text{Li}+\text{Si}$ based on numerical solution of the time-dependent Schrödinger equation for external neutrons of projectile nuclei ^6He and ^9Li yielded good agreement with experimental data.

1. Introduction

It is well known that neutron rearrangement may play an important role in nuclear reactions. The aim of this work is the investigation of the reactions with light nuclei having different external neutron shells. The experiments on measurements of total cross sections were performed for reactions $^{4,6}\text{He}+\text{Si}$ and $^{6,7,9}\text{Li}+\text{Si}$. The interesting results are the unusual wide enhancement of total cross section for $^9\text{Li}+\text{Si}$ reaction as compared with $^{6,7}\text{Li}+\text{Si}$ reactions. The similar weaker behaviour was found for $^6\text{He}+\text{Si}$ reaction as compared with $^4\text{He}+\text{Si}$ reaction. The time-dependent quantum approach combined with the optical model was used for explanation of these effects.

2. Experimental results

The experimental setup for the implementation of the transmission method using a multilayer telescope [1] is shown in figure 1. A system of silicon detectors $\Delta E_i - E$, $i = 0-4$ (Si-telescope) was surrounded by the CsI(Tl) γ -spectrometer of complete geometry for registration of γ -rays and neutrons. The thin detectors ΔE_0 , ΔE_1 were used to identify the beam particles and determine the particle flux incident on the target. The position-sensitive detector ΔE_2 was used as a so-called active collimator [2] which determined the particle flux incident on the central region of the target ΔE_3 . The detectors ΔE_4 , E were used to analyze the products of reactions occurring in the material of the target ΔE_3 .

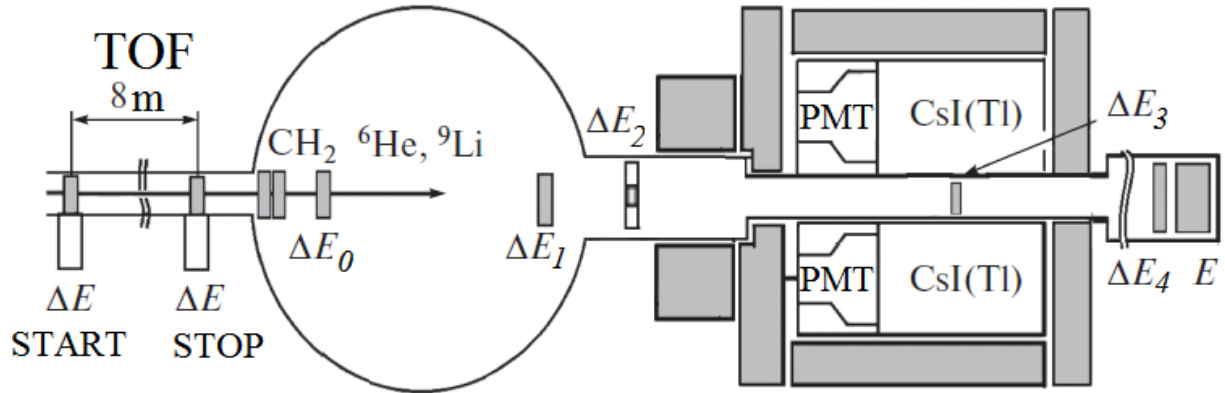


Figure 1. Schematic representation of the experimental setup for measuring the reaction cross sections by the method of the 4π scintillation γ -spectrometer.

The experiment was performed on the accelerator U400M of the Flerov Laboratory of Nuclear Reactions (FLNR), Joint Institute for Nuclear Research (JINR). To obtain the secondary beam the fragmentation reaction of ^{11}B beam with the energy $E_{lab} = 32 \text{ A MeV}$ on the target ^9Be was used. The secondary beam consisting of a mixture of particles ^6He and ^9Li was formed and purified by the magnetic system of the achromatic fragment separator ACCULINNA [3]. The beam energy was varied by a fragment separator magnetic system, the choice of the thickness of the hydrogen-containing plates of CH_2 absorbers in the range $E \approx 15\text{--}50 \text{ A MeV}$ without significant loss of intensity of the beam of particles. Identification was carried out by energy losses of particles in ΔE_0 , ΔE_1 detectors of the telescope and the time of flight. In order to reduce the energy uncertainty, detectors of different thickness (100, 380, or 500 microns) were used in the experiment depending on the beam energy. Detectors of γ -spectrometer recorded γ -quanta and neutrons in coincidence with the start signal from the detector ΔE_1 . The number of events of the reaction was determined from the analysis of energy losses in natural Si-target as well as the analysis of gamma and neutron radiation detected by the spectrometer.

The results of measurements of total cross sections for reactions $^{6,7,9}\text{Li} + \text{Si}$ and $^{4,6}\text{He} + \text{Si}$ are presented in figure 2. Filled symbols are the results of measurements by various methods performed in FLNR, JINR; open symbols are experimental data of other authors. Two peculiarities of the energy dependence of the total cross sections for the reactions with neutron-rich nuclei can be observed in the experimental data. The first peculiarity is the increased cross section for the reaction with the neutron-rich halo nucleus ^6He with respect to its core ^4He in the whole studied energy range. The second peculiarity is the local increase of the values of the cross section in the form of a bump in a limited energy range $10\text{--}30 \text{ A MeV}$ for the case of $^9\text{Li} + \text{Si}$. The first peculiarity may be explained by the larger size of the ^6He nucleus, while the second peculiarity may be a manifestation of the dynamic effects associated with rearrangement of external weakly bound nucleons or their clusters in the ^9Li nucleus.

The analysis of these effects using the microscopic complex folding potential in Ref. [10] as well as within the optical model in Ref. [11] did not provide satisfactory explanation of the observed features in the behaviour of the energy dependence of the total cross section. In this study, the potentials of the optical model were modified to take into account the dynamic rearrangement of two external neutrons of projectile nuclei ^6He and ^9Li .

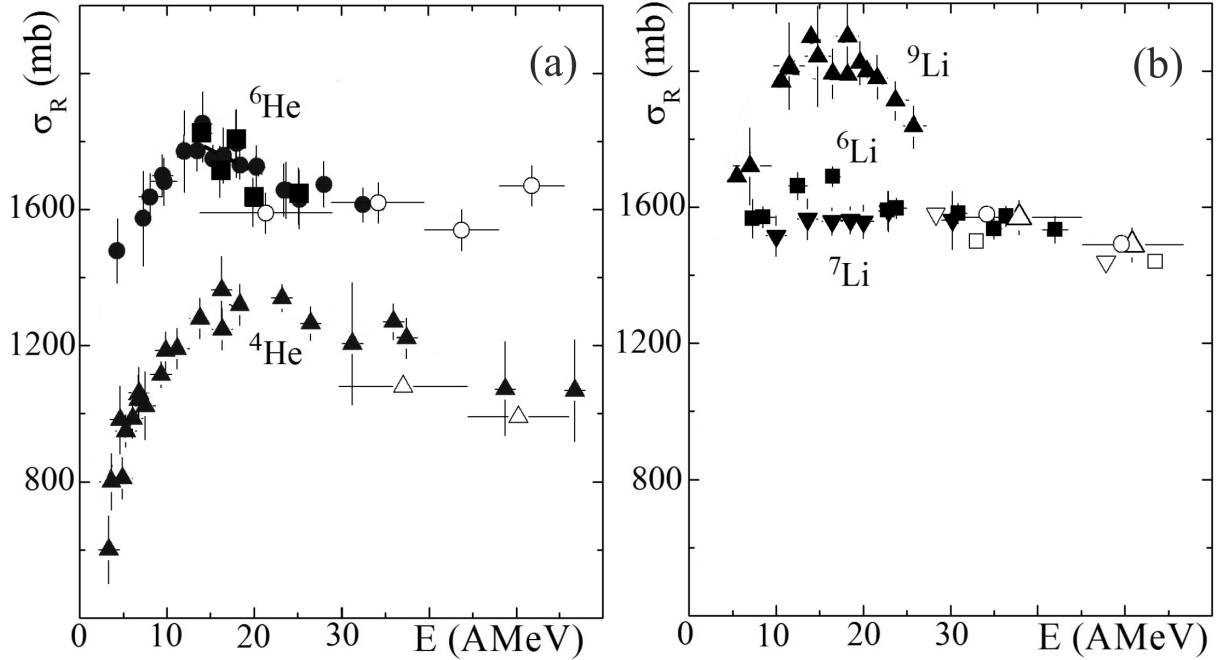


Figure 2. The total cross sections for the reactions $^{4,6}\text{He}+\text{Si}$ (a) and $^{6,7,9}\text{Li}+\text{Si}$ (b) as a function of the energy of the incident particles. Symbols are the experimental data from Refs. [1, 4–9].

3. Theoretical analysis

The presence of two external neutrons forming a weakly bound neutral cluster (dineutron) is common for the most probable configurations of nuclei ^6He ($\alpha + n + n$) and ^9Li ($\alpha + t + n + n$). In a simplified approximation, neutrons can be regarded as moving independently in the mean field of the shell model. The rearrangement of external neutrons between the projectile nucleus and the target nucleus, for example, their presence with a high probability between the surfaces of the colliding nuclei, can significantly enhance the mutual attraction of the nuclei and lead to an increase in the total cross section of the reaction.

For theoretical description of neutron rearrangement during collisions of heavy atomic nuclei we used the time-dependent Schrödinger equation (TDSE) approach [12–14] for the external neutrons combined with the classical equations of motion of atomic nuclei. The evolution of the components ψ_1, ψ_2 of the spinor wave function $\Psi(\vec{r}, t)$ for the neutron with the mass m during the collision of nuclei is determined by equation (1) with the operator of the spin-orbit interaction $\hat{V}_{LS}(\vec{r}, t)$

$$i\hbar \frac{\partial}{\partial t} \Psi(\vec{r}, t) = \left\{ -\frac{\hbar^2}{2m} \Delta + W(\vec{r}, t) + \hat{V}_{LS}(\vec{r}, t) \right\} \Psi(\vec{r}, t). \quad (1)$$

The centres of nuclei $\vec{r}_1(t), \vec{r}_2(t)$ with the masses m_1, m_2 move along classical trajectories. We may assume that before contact of the surfaces of spherical nuclei with the radii R_1, R_2 the potential energy of a neutron is equal to the sum of its interaction energies with both nuclei. The initial conditions for the wave functions were obtained based on the shell model calculations with the parameters providing neutron separation energies close to the experimental values.

Examples of the evolution of the probability density of the external neutrons of ^9Li nucleus when colliding with the nucleus ^{28}Si at different energies are shown in figure 3. During a slow (adiabatic) relative motion of the colliding nuclei the external neutrons (dineutron cluster) of

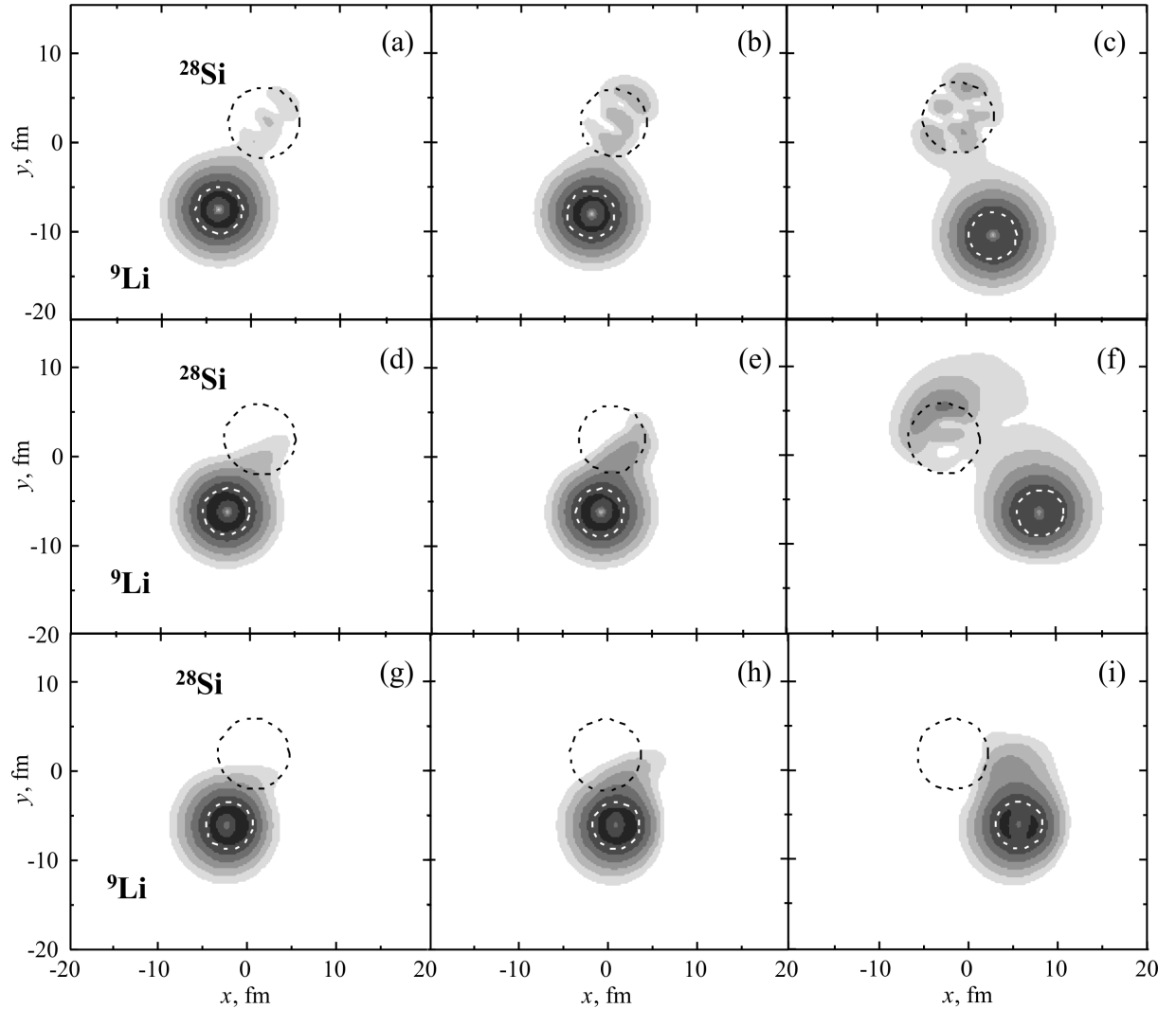


Figure 3. Examples of the evolution of the probability density of external neutrons of the ${}^9\text{Li}$ nucleus during the collision with the ${}^{28}\text{Si}$ nucleus at energies $E_{\text{lab}} = 2 \text{ A MeV}$ ((a), (b), (c), $\gamma = 0.24$, adiabatic regime), 15 A MeV ((d), (e), (f), $\gamma = 0.7$, intermediate regime), and 60 A MeV ((g), (h), (i), $\gamma = 1.4$, diabatic regime). The course of time corresponds to the panel locations from left to right.

${}^9\text{Li}$ nucleus are penetrating the ${}^{28}\text{Si}$ nucleus and populating the slowly changing two-centre (“molecular”) states, the probability density for which fills a large part of the volume of the target nucleus. During the rapid (diabatic) relative motion the probability density of neutrons does not have time to fill all the target nucleus and its change is more local. After the separation of the nuclei the wave packet in the surface region of the target nucleus remains spreading and rotating with large angular momentum. At intermediate velocities there is a transition from the adiabatic regime to the diabatic one.

The qualitative character of the rearrangement of external neutrons during the approach of nuclei depends on the ratio of the average velocity $\langle v \rangle$ of the external neutron and the relative velocity v_{rel} of the nuclei in the process of collision. The average kinetic energy $\langle \varepsilon \rangle$ of external weakly bound neutrons in the nuclei ${}^6\text{He}$ and ${}^9\text{Li}$ may be approximately calculated within the

shell model. Using estimation $v_{\text{rel}} \approx v_1 = \sqrt{2E_{\text{lab}}/m_1}$, where E_{lab} is the energy of the projectile nucleus with the mass $m_1 = Am_0$, m_0 is the atomic mass unit, we obtain the ratio of velocities

$$\frac{v_1}{\langle v \rangle} \approx \gamma \equiv \left(\frac{E_{\text{lab}}}{\langle \varepsilon \rangle A} \right)^{1/2}. \quad (2)$$

At low energies, when $\langle v \rangle \gg v_1$, $\gamma \ll 1$, during the flight of the projectile nucleus close to the target nucleus the weakly bound neutrons may, relatively speaking, make many turns around the cores of both nuclei. In the extremely diabatic case (at intermediate energies), when $\langle v \rangle \ll v_1$, $\gamma \gg 1$, the neutron may not be able to move to the target nucleus during the time of flight. The value of the parameter γ may be used to estimate the degree of adiabaticity of the collision.

The real part of the potential $\bar{V}(R)$ for nuclei with “frozen” neutrons was supplemented with the diabatic correction arising from an increase in neutron probability density between the surfaces of the nuclei as they approach

$$V_{\text{d}}(R, E_{\text{lab}}) = \bar{V}(R) + \eta(E_{\text{lab}}) \delta V_{\text{d}}(R, E_{\text{lab}}) \quad (3)$$

with the function $\delta V_{\text{d}}(R(t), E_{\text{lab}})$

$$\delta V_{\text{d}}(R(t), E_{\text{lab}}) = \int_{\Omega} d^3 r_3 \delta \rho_1(r_3, t) U_{\text{T}}(|\vec{r}_3 - \vec{r}_2(t)|), \quad (4)$$

where $U_{\text{T}}(r)$ is the mean field for neutrons in the target nucleus, $\delta \rho_1(r_1, t) = \rho_1(r_1, t) - \rho_1^{(0)}(r_1)$, $\rho_1(r_1, t)$ is the probability density of the external neutrons of the projectile nucleus, $\rho_1^{(0)}(r_1)$ is the same density calculated in the absence of interaction of these neutrons with the target nucleus, Ω is the region between the surfaces of the nuclei,

$$\eta(E_{\text{lab}}) = \frac{1}{1 + \exp \left[\frac{1}{\alpha} \left(\langle \varepsilon \rangle - \left(\frac{E_{\text{lab}}}{A} \right) \right) \right]} \quad (5)$$

with the variable parameters $\langle \varepsilon \rangle \approx 10$ MeV determining the position $\bar{E}_{\text{lab}} = \langle \varepsilon \rangle A$ of the transition region and $\alpha \approx 2$ MeV determining its width. The diabatic correction $\delta V_{\text{d}}(R, E_{\text{lab}})$ reduces the height $B(E_{\text{lab}})$ and shifts to the right the position $R_B(E_{\text{lab}})$ of the Coulomb barrier

$$R_B(E) = R_{B,0} + \delta R_B(E). \quad (6)$$

For the imaginary part of the potential, we used the approximation with the exponential dependence

$$W(r) = \begin{cases} -W_1, r < R_b \\ W_1 \exp \left(-\frac{r-R_b}{b} \right), r \geq R_b \end{cases} \quad (7)$$

and the radius R_b increasing together with the shift of the barrier position

$$R_b(E) = R_a + k \delta R_B(E), \quad (8)$$

where $b = 1$ fm, $k = 2$, $R_a = 5.8$ fm for the reaction ${}^9\text{Li} + {}^{28}\text{Si}$. In the case of reactions with nuclei ${}^4\text{He}$, ${}^7\text{Li}$, for the real and the imaginary parts of the nuclear potential the Woods-Saxon form was used

$$\text{Re} \{V_{\text{N}}(R)\} \equiv V(R) = -V_0 [1 + \exp((R - R_V)/a_V)]^{-1}, \quad (9)$$

$$\text{Im} \{V_{\text{N}}(R)\} \equiv W(R) = -W_0 [1 + \exp((R - R_W)/a_W)]^{-1}. \quad (10)$$

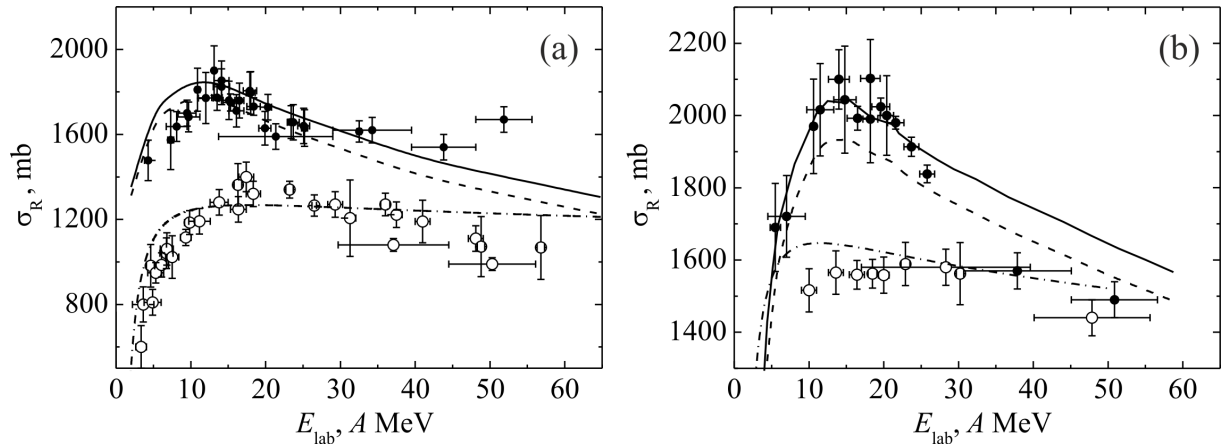


Figure 4. The total cross sections for reactions $^{4,6}\text{He} + ^{28}\text{Si}$ (a) and $^{7,9}\text{Li} + ^{28}\text{Si}$ (b), symbols are the experimental data from Refs. [1, 4–9]: $^{6}\text{He} + ^{28}\text{Si}$ and $^{9}\text{Li} + ^{28}\text{Si}$ (filled circles), $^{4}\text{He} + ^{28}\text{Si}$ and $^{7}\text{Li} + ^{28}\text{Si}$ (empty circles), curves are the results of calculation within the optical model with the potentials (3), (7): (a) for $R_a = 5.0$ fm (solid line) and $R_a = 4.8$ fm (dashed line), (b) for $R_a = 5.8$ fm (solid line) and $R_a = 5.6$ fm (dashed line); dash-dotted lines are the results of calculations with the potentials (9), (10) for the reactions $^4\text{He} + ^{28}\text{Si}$ (a) and $^7\text{Li} + ^{28}\text{Si}$ (b).

For collisions $^{6,7}\text{Li} + ^{28}\text{Si}$, the parameters of the potential were obtained by fitting the angular distributions for elastic scattering of $^{6,7}\text{Li}$ on ^{28}Si at several collision energies with the initial approximation in the Akyüz-Winther parametrization [15]. It should be mentioned that for a wide energy range the same values of the parameters of the optical potential were obtained. Because of the absence of experimental data on elastic scattering of ^9Li on ^{28}Si , the parameters for the reaction $^9\text{Li} + ^{28}\text{Si}$ were obtained by extrapolation of the parameters for $^{6,7}\text{Li} + ^{28}\text{Si}$. Similarly, because of the absence of experimental data on elastic scattering of $^{4,6}\text{He}$ on ^{28}Si , the values of the parameters for reactions $^{4,6}\text{He} + ^{28}\text{Si}$ were found by extrapolation of the values of the parameters obtained by fitting experimental differential cross sections for the elastic scattering of $^{4,6}\text{He}$ on ^{12}C .

4. Results and discussion

The results of calculation of the total cross section for reactions $^{4,6}\text{He} + ^{28}\text{Si}$ and $^{6,7,9}\text{Li} + ^{28}\text{Si}$ are shown in figure 4. As can be seen, they are in good agreement with the experimental data in the whole energy range. Thus, the calculations indicated a possible reason for the manifestation of the enhancement of the total cross sections for reactions $^{6}\text{He} + ^{28}\text{Si}$ and $^{9}\text{Li} + ^{28}\text{Si}$. It consists in the formation of a region of increased neutron density between the surfaces of the nuclei during the entire time of the collision. This increases the attraction of the nuclei, shifts the position of the barrier toward higher values, and increases the size of the region where processes leading to an exit from the elastic channel take place with considerable probability. Within the framework of the optical model, the total contribution of such processes is taken into account by the imaginary part of the potential and the dependence on the energy of its parameters: radius and/or diffuseness. The smaller manifestation of the local maximum in the energy dependence of the cross section for the ^6He nucleus in comparison with ^9Li can be explained by the greater extent and sparseness of the neutron halo of the ^6He nucleus compared to the more compact neutron layer (skin) of the ^9Li nucleus.

5. Conclusions

In this paper we presented experimental results of a direct measurement of the total cross sections for the reactions $^{4,6}\text{He} + \text{Si}$ and $^{6,7,9}\text{Li} + \text{Si}$ in the beam energy range 5–50 A MeV. The enhancements of the total cross sections for reactions $^6\text{He} + \text{Si}$ and $^9\text{Li} + \text{Si}$ have been observed. The theoretical analysis of the possible causes of these effects in the collisions of nuclei ^6He and ^9Li with Si nuclei was performed including the influence of external neutrons of weakly bound projectile nuclei. The time-dependent model proposed in the paper shows that the rearrangement of external weakly bound neutrons of nuclei ^6He and ^9Li during the collision changes the real and the imaginary parts of the interaction potential, which may cause a local enhancement in the total reaction cross sections. This enhancement is most noticeable in the range of energies where the relative velocity of the nuclei is close in magnitude to the average velocity of external neutrons of the studied light weakly bound nuclei.

Acknowledgments

We express our deep gratitude to the team of researchers of the ACCULINNA experimental facility (FLNR, JINR) as well as to the team of the U400M accelerator (FLNR, JINR) for maintenance of experiments. We also thank A S Denikin and A V Karpov for fruitful discussions. The work was supported by Russian Science Foundation (RSF), grant No. 17-12-01170.

References

- [1] Sobolev Yu G *et al* 2005 Energy dependence of total reaction cross section for $^{4,6}\text{He}$, $^7\text{Li} + ^{28}\text{Si}$ interaction at $E = 5\text{--}50$ MeV/nucleon *Bull. Russ. Acad. Sci.: Phys.* **69** 1790–5
- [2] Sobolev Yu G, Ivanov M P, Kondratiev N A and Penionzhkevich Yu E 2011 Active collimators in experiments with exotic nuclear beams *Instr. Exp. Techn.* **54** 449
- [3] Rodin A M *et al* 2003 Status of ACCULINNA beam line *Nucl. Instr. Meth. Phys. Res. B* **204** 114–8
- [4] Ugryumov V Yu *et al* 2005 Energy dependence of the total cross section for the reaction of ^4He ions with silicon nuclei *Phys. Atom. Nucl.* **68** 16–20
- [5] Sobolev Yu G *et al* 2017 Experimental study of the energy dependence of the total cross section for the $^6\text{He} + ^{nat}\text{Si}$ and $^9\text{Li} + ^{nat}\text{Si}$ reactions *Phys. Part. Nucl.* **48** 922–6
- [6] Warner R E *et al* 1996 Total reaction and 2n-removal cross sections of 20–60 A MeV $^{4,6,8}\text{He}$, $^{6-9,11}\text{Li}$, and ^{10}Be on Si *Phys. Rev. C* **54** 1700–9
- [7] Warner R E *et al* 2006 Reaction and proton-removal cross sections of ^6Li , ^7Be , ^{10}B , $^{9,10,11}\text{C}$, ^{12}N , $^{13,15}\text{O}$, and ^{17}Ne on Si at 15 to 53 MeV/nucleon *Phys. Rev. C* **74** 014605
- [8] Ingemarsson A *et al* 2000 New results for reaction cross sections of intermediate energy α -particles on targets from ^9Be to ^{208}Pb *Nucl. Phys. A* **676** 3–31
- [9] Penionzhkevich Yu E, Sobolev Yu G, Samarin V V and Naumenko M A 2017 Peculiarities in total cross sections of reactions with weakly bound nuclei ^6He , ^9Li *Phys. Atom. Nucl.* **80** 928–41
- [10] Lukyanov K V, Zemlyanaya E V, Lukyanov V K, Kukhtina I N, Penionzhkevich Yu E and Sobolev Yu G 2008 Microscopic analysis of the energy dependence of the ^6He , $^6\text{Li} + ^{28}\text{Si}$ total reaction cross sections in the energy range $E = 5\text{--}50$ A MeV *Bull. Russ. Acad. Sci.: Phys.* **72** 356–60
- [11] Kabdrakhimova G D, Sobolev Yu G, Kukhtina I N, Kuterbekov K A, Mendibaev K O and Penionzhkevich Yu E 2017 Investigation of total cross sections for reactions induced by ^6He interaction with silicon nuclei at energies between 5 and 50 MeV/A *Phys. Atom. Nucl.* **80** 32–7
- [12] Samarin V V and Samarin K V 2012 Dynamic tunnel effect at low-energy nuclear reactions with neutron-rich nuclei *Bull. Russ. Acad. Sci.: Phys.* **76** 450–3
- [13] Naumenko M A, Samarin V V, Penionzhkevich Yu E and Skobelev N K 2016 Near-barrier neutron transfer in reactions with ^3He nucleus *Bull. Russ. Acad. Sci.: Phys.* **80** 264–72
- [14] Naumenko M A, Samarin V V, Penionzhkevich Yu E and Skobelev N K 2017 Near-barrier neutron transfer in reactions $^6\text{He} + ^{45}\text{Sc}$, ^{64}Zn , and ^{197}Au *Bull. Russ. Acad. Sci.: Phys.* **81** 710–6
- [15] Winther A 1994 Grazing reactions in collisions between heavy nuclei *Nucl. Phys. A* **572** 191–235